

Supporting Information

Selective Lithium Extraction from Brine via Chemical Reduction of Iron Phosphate with
Aqueous Iron Compounds

Jing Wang,^a Alex W. Hawkins,^a Amin T. Saasi,^a Caroline G. Morin,^a Geoffrey M. Geise^a, Gary
M. Koenig Jr.^{a*}

^aDepartment of Chemical Engineering, University of Virginia, 385 McCormick Road,
Charlottesville, VA, USA 22904-4741

Table S1. Simulated brine composition with high Li⁺ concentration and 1:1 molar ratio of target Li⁺:M⁺²⁺, cations (M = K⁺, Na⁺, Mg²⁺). Chemicals listed in their order of addition.

Order of addition	Chemicals	Simulated Brine (EDTA, Li ⁺ :M ⁺²⁺ 1:1)	Simulated Brine (Citrate, Li ⁺ :M ⁺²⁺ 1:1)
1	DI Water		Y g
2	Acetic acid solution (1 M)	X g	
3	EDTA	0.1 M	
4	LiOH	1.3 M, pH to ~7	
5	Potassium Citrate		0.1 M
6	MCl (K ⁺ , Na ⁺ , Mg ²⁺)	1.3 M	1 M
7	LiCl		1 M
8	FeCl ₂ • 4H ₂ O	0.1 M	0.1 M
9	FP	0.5 g	0.5 g
	Total	100 g	100 g

“X” and “Y” were part of the baseline solution during preparation of the brine. These amounts were determined after subtracting the mass intended for all the other chemicals, and the mass of each chemical was calculated based on a targeted volume of 0.1 L of brine. The total mass of brine was 100 g. Due to the different mass of competing cations (M), the mass of the baseline solution (X or Y) slightly varied. The mass ranges for X and Y in the prepared solutions was 78-90 g and 80-90 g, respectively.

Table S2. Simulated brine composition to match the $\text{Li}^+:\text{Na}^+$ molar ratio representative of the Salton Sea (1:78).¹ Chemicals listed in their order of addition.

Order of addition	Chemicals	Simulated Brine (EDTA, $\text{Li}^+:\text{Na}^+$ 1:78)	Simulated Brine (Citrate, $\text{Li}^+:\text{Na}^+$ 1:78)
1	DI water		Y g
2	Acetic acid solution (1M)	X g	
3	EDTA	15, 30, 50, 100, 200, 300 mM	15, 30, 50, 100 mM
4	KOH	Add until pH ~7	
5	NaCl	3.04 M	3.04 M
6	LiCl	0.039 M	0.039 M
7	$\text{FeCl}_2 \cdot 4\text{H}_2\text{O}$	15, 30, 50, 100, 200, 300 mM	15, 30, 50, 100 mM
8	FP	0.5 g	0.5 g
	Total	100 g	100 g

“X” and “Y” were part of the baseline solution during preparation of the brine. These amounts were determined after subtracting the mass intended for all the other chemicals, and the mass of each chemical was calculated based on a targeted volume of 0.1 L of brine. The total mass of brine was 100 g. Due to the different mass of the redox mediator, EDTA- Fe^{2+} and Citrate- Fe^{2+} , the mass of the baseline solution (X or Y) slightly varied. The mass ranges for X and Y in the prepared solutions was 70-80 g and 70-84 g, respectively.

Table S3. Composition for brine prepared to be more representative of discharge from geothermal power plants at the Salton Sea.¹

Chemicals	Mass (g) Mediator: EDTA-Fe ²⁺	Mass (g) Mediator: Citrate-Fe ²⁺
Potassium Citrate	-	3.24
EDTA	2.92	-
KOH	7.4	-
FeCl ₂ • 4H ₂ O	0.6	0.6
KCl	3.41	3.41
LiCl	0.14	0.14
MnCl ₂ • 4H ₂ O	0.75	0.75
NaCl	15.1	15.1
Boric Acid	0.25	0.25
FeCl ₂ • 4H ₂ O	1.98	1.98
Water	67.5	74.5
Total	100	100

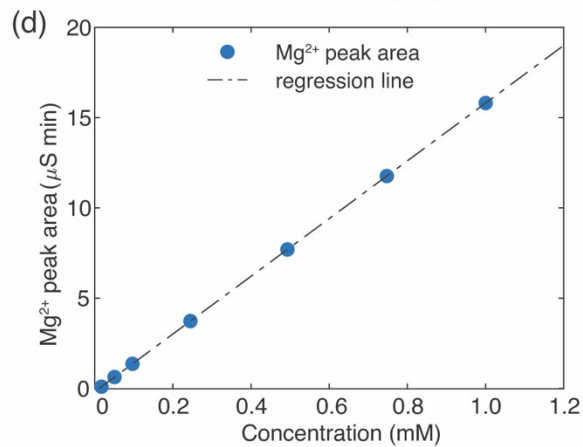
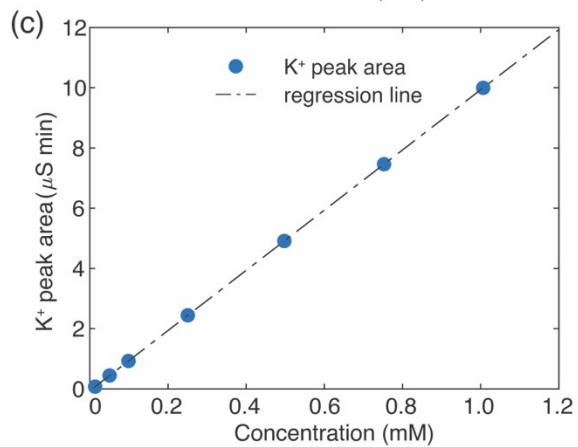
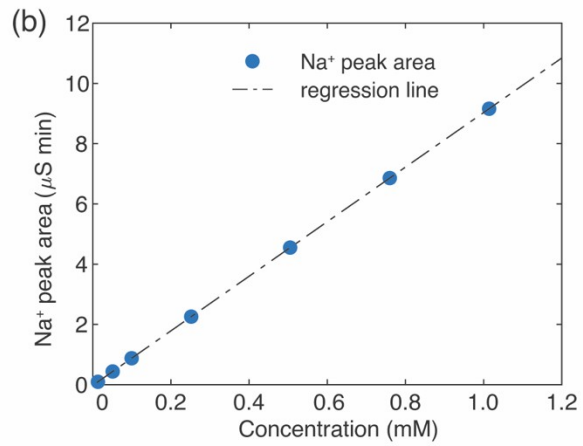
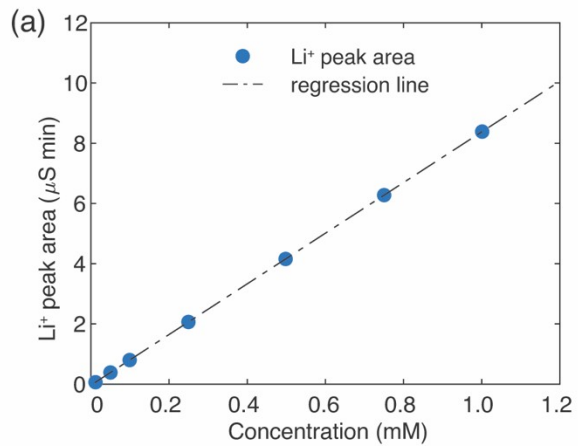


Figure S1. Calibration curves for peak area as a function of prepared cation concentration using ion chromatography. (a) Li^+ , (b) Na^+ , (c) K^+ , and (d) Mg^{2+} are shown, and the solutions containing these cations were prepared as chloride salts. The targeted solution concentration range was 0.01 to 1 mM.

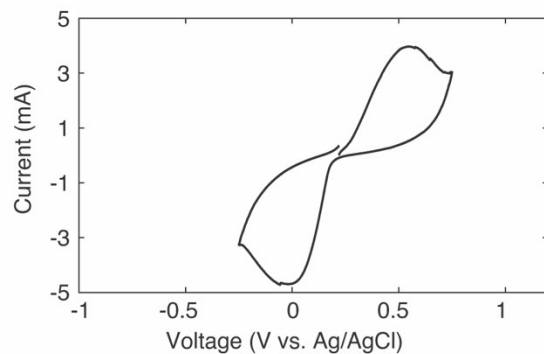


Figure S2. Cyclic voltammogram for LFP material as the working electrode measured in 1 M Li_2SO_4 solution. The scan range was -0.25 V to 0.75 V (vs. Ag/AgCl), and the scan rate was 0.2 mV s^{-1} .

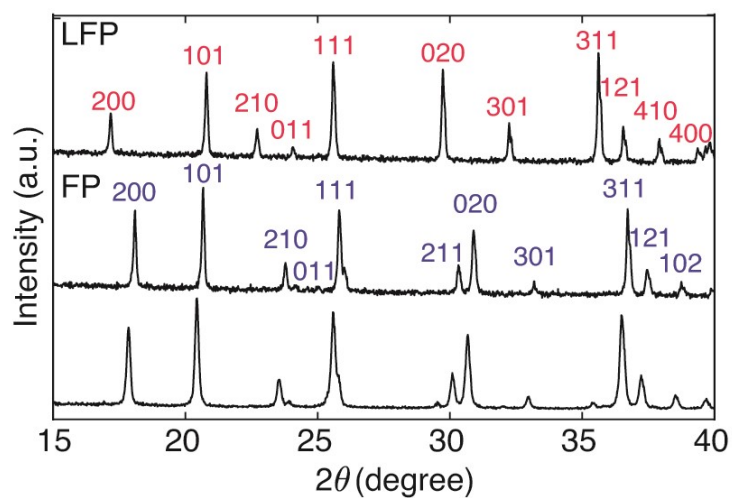


Figure S3. XRD pattern (bottom) for FP reduced in 1 M of LiCl solution at 75 °C for 24 hours with 0.1 M of FeCl₂ and no added ligands. XRD for LFP (top) and FP (middle) powders also provided.

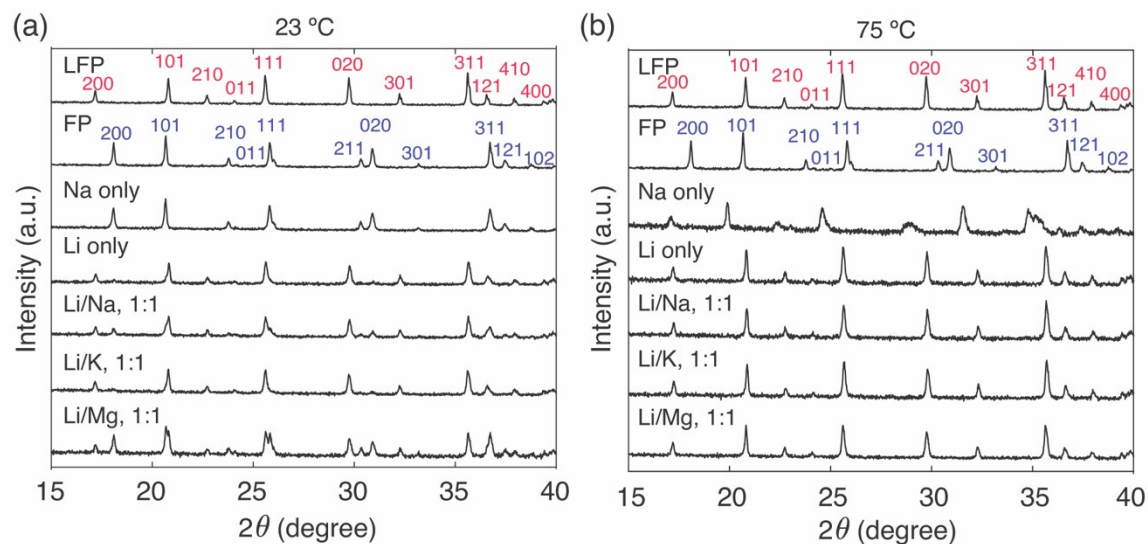


Figure S4. XRD patterns for FP powder after chemical reduction at (a) 23 °C and (b) 75 °C in brine solutions using EDTA-Fe²⁺ redox mediators. Each monovalent cation concentrations in the brine were ~1.3 M, and the molar ratios of the cations in the brine are indicated on the Figure. At the top of each Figure are the patterns for the as received LFP powder and the LFP powder after chemical oxidation with hydrogen peroxide to form FP.

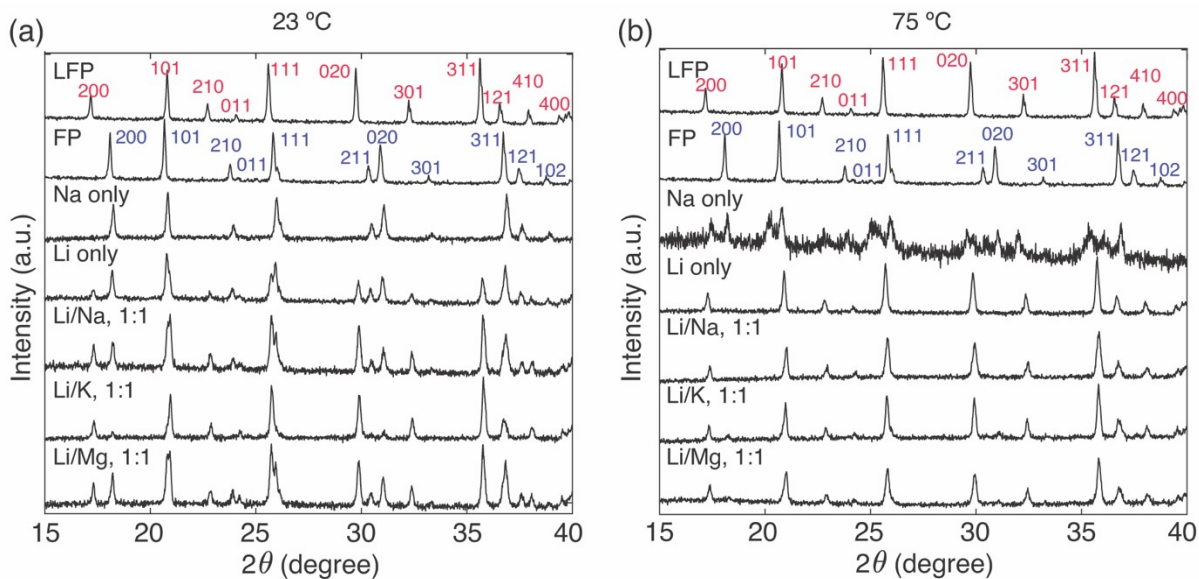


Figure S5. XRD patterns for FP powder after chemical reduction at (a) 23 °C and (b) 75 °C using brine solutions containing Citrate-Fe²⁺ redox mediators. Each monovalent cation concentrations in the brine were ~1 M, and the molar ratios of the cations in the brine are indicated on the Figure. At the top of the Figure are the patterns for the as received LFP powder and the LFP powder after chemical oxidation with hydrogen peroxide to form FP.

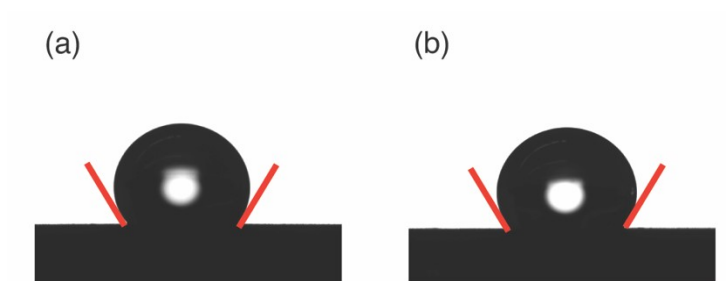


Figure S6. Example droplet images for determining contact angle of 1:78 $\text{Li}^+:\text{Na}^+$ brine solution with 0.1 M of redox mediator (a) Citrate- Fe^{2+} and (b) EDTA- Fe^{2+} on FP composite electrode.

Table S4. Comparison of Li⁺ adsorption capacity, selectivity, and energy consumption with reported literature using electrochemical methods for Li⁺ extraction from brine.

System	Li ⁺ /Na ⁺ concentration	Total cations concentration in the brine source (g/L)	Selectivity factor α_{Na}^{Li}	Capacity (mg Li ⁺ g ⁻¹)	Energy (Wh mol ⁻¹)	Ref
FP/LFP	0.1 M Li ⁺ / 4.2 M Na ⁺	113	479	30	-	2
LFP/Ag	0.05 M Li ⁺ / 5 M Na ⁺	115	548	7.76	1±0.6	3
Li _{1-x} FePO ₄ /C	0.005 M Li ⁺ / 0.05 M Na ⁺	1.2	-	21	3.03±0.5	4
LFP/FP	0.004 M Li ⁺ / 0.03 M Na ⁺	1.44	70.63	17.1	-	5
LFP/C/ K ₂ MFe(CN) ₆	0.004 M Li ⁺ / 0.03 M Na ⁺	1.44	-	26.75	22.21	6
LiFePO ₄ / NiHCF	0.0019 M Li ⁺ / 0.011 M Na ⁺	1.01	-	13	8.7	7
LFP/AEM/F P	0.07 M Li ⁺ / 4 M Na ⁺	92.5	138	27	-	8
LFP/Pt	0.2 M Li ⁺ / 4.5 M Na ⁺	105	210.5	14.62	0.768	9
NMC/Ag	0.2 M Li ⁺ / 2.6 M Na ⁺	109	770	10.8	2.6	10
Pt/MnO ₂	0.0007 M Li ⁺ / 0.046 M Na ⁺	1.26	-	11	-	11
LiMn ₂ O ₄ / Li _{1-x} Mn ₂ O ₄	0.021 M Li ⁺ / 0.33 M Na ⁺	9	320	21	18	12
HTO (RGO- TA)/C	0.2 M Li ⁺ / 2.75 M Na ⁺	64.7	57	25.2	-	13
LFP/ Citrate-Fe ²⁺	0.039 M Li ⁺ / 3.04 M Na ⁺	83	380	14	0	This work
LFP/ EDTA-Fe ²⁺	0.039 M Li ⁺ / 3.04 M Na ⁺	83	60	14	0	This work
[-]: data are not reported in the work.						

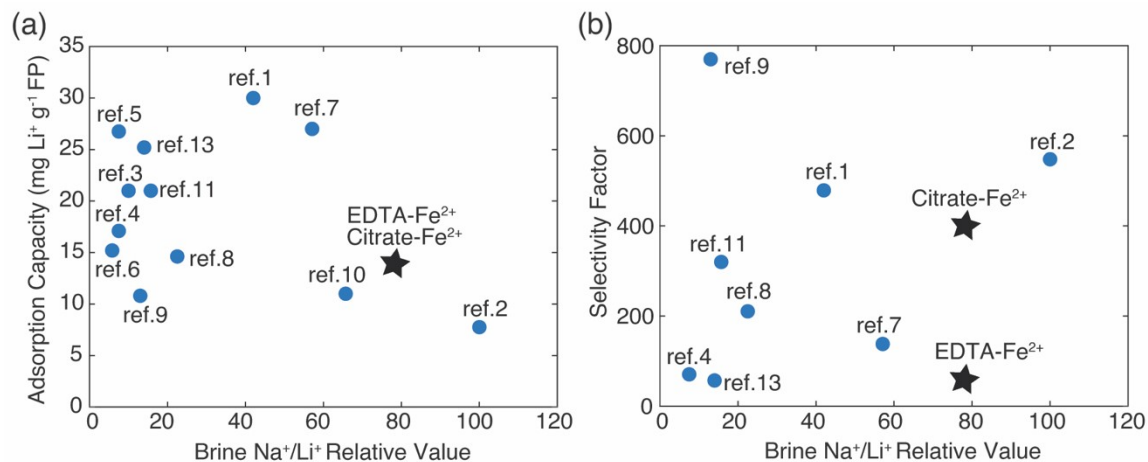


Figure S7. (a) Li⁺ adsorption capacity and (b) Li⁺ selectivity factor for this work (black stars) and previous reports (blue dots, from Refs. 2-13). In most cases, adsorption capacity was converted to the same unit basis from the reported data and Li⁺ selectivity factor was recalculated based on Eqn. 1 in main text.

References

- 1 S. Ventura, S. Bhamidi, M. Hornbostel and A. Nagar, *Calif. Energy Comm.*, 2020, CEC-500-2020-020.
- 2 W. Xu, D. Liu, X. Liu, D. Wang, L. He and Z. Zhao, *Desalination*, 2022, **546**, 116188.
- 3 M. Pasta, A. Battistel and F. La Mantia, *Energy Environ. Sci.*, 2012, **5**, 9487–9491.
- 4 L. Wang, K. Frisella, P. Srimuk, O. Janka, G. Kickelbick and V. Presser, *Sustain. Energy Fuels*, 2021, **5**, 3124–3133.
- 5 S. Sun, X. Yu, M. Li, J. Duo, Y. Guo and T. Deng, *J. Clean. Prod.*, 2020, **247**, 119178.
- 6 T. Han, X. Yu, Y. Guo, M. Li, J. Duo and T. Deng, *Electrochim. Acta*, 2020, **350**, 136385.
- 7 R. Tröcoli, A. Battistel and F. La Mantia, *ChemSusChem*, 2015, **8**, 2514–2519.
- 8 J. Xiong, L. He and Z. Zhao, *Desalination*, 2022, **535**, 115822.
- 9 M. Du, J.-Z. Guo, S.-H. Zheng, Y. Liu, J.-L. Yang, K.-Y. Zhang, Z.-Y. Gu, X.-T. Wang and X.-L. Wu, *Chinese Chem. Lett.*, 2022, **34**, 107706.
- 10 C. P. Lawagon, G. M. Nisola, R. A. I. Cuevas, H. Kim, S. P. Lee and W. J. Chung, *Chem. Eng. J.*, 2018, **348**, 1000–1011.
- 11 H. Kanoh, K. Ooi, Y. Miyai and S. Katoh, *Sep. Sci. Technol.*, 1993, **28**, 643–651.
- 12 M. Y. Zhao, Z. Y. Ji, Y. G. Zhang, Z. Y. Guo, Y. Y. Zhao, J. Liu and J. S. Yuan, *Electrochim. Acta*, 2017, **252**, 350–361.
- 13 J. Zhang, Z. Cheng, X. Qin, X. Gao, R. Yun and X. Xiang, *ACS Appl. Mater. Interfaces*, 2023, **15**, 29586–29596.